The transient response of atmospheric and oceanic heat transports to anthropogenic warming

Chengfei He 1,2,3*, Zhengyu Liu 2* and Aixue Hu 44

Model projections of the near-future response to anthropogenic warming show compensation between meridional heat transports by the atmosphere (AHT) and ocean (OHT) that are largely symmetric about the equator 1-3, the causes of which remain unclear. Here, using both the Coupled Model Intercomparison Project Phase 5 archive and Community Climate System Model version 4 simulations forced with Representative Concentration Pathway 8.5 to 2600, we show that this transient compensation—specifically during the initial stage of warming—is caused by combined changes in both atmospheric and oceanic circulations. In particular, it is caused by a southward OHT associated with a weakened Atlantic Meridional Overturning Circulation, a northward apparent OHT associated with an ocean heat storage maximum around the Southern Ocean, and a symmetric coupled response of the Hadley and Subtropical cells in the Indo-Pacific basin. It is further shown that the true advective OHT differs from the fluxinferred OHT in the initial warming due to the inhomogeneous responses of ocean heat storage. These results provide new insights to further our understanding of future heat transport responses, and thereby global climatic processes such as the redistribution of ocean heat.

The combined atmospheric (AHT) and oceanic (OHT) meridional heat transports, peaking at $5.5\,\mathrm{PW}$ ($1\,\mathrm{PW}=10^{15}\,\mathrm{W}$) near $35^{\circ}\,\mathrm{N/S}$ (Supplementary Fig. 1a), are a fundamental ingredient of the climate system that connects climate processes across the globe^{4,5}. The mechanism behind the response of the heat transports to global warming has been studied previously¹⁻³. However, little attention has been paid to the role of the ocean in determining the initial transient response of AHT and OHT to global warming in the coming century.

Current modelling studies of this initial response to global warming suggest a compensated change of AHT and OHT that is largely symmetric about the equator, with an increasing poleward AHT and decreasing poleward OHT in both hemispheres ^{1,2,6}. This symmetric and compensated response is puzzling for several reasons. In principle, in the absence of a change in both the net radiation flux at the top of the atmosphere (TOA) and the oceanic heat storage, the responses of AHT and OHT should be in the opposite directions as a compensation response ⁷⁻¹⁰. However, first, in almost all of the previous studies, the OHT response is inferred from the surface heat flux (OHT_{FX})¹⁻³ (see Methods), which equals the true advective OHT (OHT_{VT}; see Methods) only if the oceanic response

is in quasi-equilibrium such that the contribution of heat storage to the oceanic heat budget is negligible. Yet, in the initial stage of global warming, ocean heat storage increases significantly, accounting for more than 90% of the total heat uptake 11,12; therefore, OHT $_{\rm FX}$ could differ significantly from OHT $_{\rm VT}$. Therefore, what is the role of heat storage in the heat transport response? Second, in theory, the global warming forcing perturbs radiative fluxes at both the TOA and the Earth surface, with no clear dominance in the net effect on heat transport 9 . Why do AHT and OHT exhibit a robust compensation response? Finally, the symmetric response contradicts the heat transport response induced by the robust weakening of the Atlantic Meridional Overturning Circulation (AMOC) under global warming $^{13-15}$, which should exhibit an inter-hemispherically asymmetric heat transport response across the equator $^{16-18}$. Why, then, is the initial response still largely symmetric?

Here, we study the mechanism for the initial response of the heat transport to global warming from the ocean perspective, with an emphasis on the role of ocean heat storage and coupled ocean—atmosphere dynamics. Our study suggests that the largely symmetric $\mathrm{OHT}_{\mathrm{FX}}$ responses in the initial warming stage can be viewed as a cancellation between a southward OHT response associated with the weakening AMOC and an apparent northward OHT associated with the inhomogeneous increase of ocean heat content ($\mathrm{OHT}_{\mathrm{HC}}$) see Methods), such that the symmetric compensation response in AHTs and OHTs is primarily manifested by the coupled responses of the atmospheric Hadley Cell and the oceanic Subtropical Cell (STC) in the tropical and subtropical regions (the Hadley Cell–STC hereafter).

To examine the meridional heat transport response in different stages of global warming from 1850–2600, we examined historical and Representative Concentration Pathway 8.5 (RCP8.5) scenarios from the National Center for Atmospheric Research (NCAR) Community Climate System Model version 4 (CCSM4; see Methods)¹⁹. We specifically focused on the transient responses of AHT and OHT during the twenty-first century (2006–2100) in CCSM4, which are shown alongside other model simulation results, such as those of the Community Earth System Model (CESM) Large Ensemble (CESM-LE)²⁰ and Coupled Model Intercomparison Project Phase 5 (CMIP5; see Methods)²¹.

During the initial warming of the twenty-first century (Fig. 1a), AHT increases poleward in both hemispheres, and this increase is compensated for almost everywhere by a decrease in OHT_{FX} , which appears to be largely symmetric about the equator (Figs. 1a and 2b),

¹College of Atmospheric Sciences, Nanjing University of Information Science and Technology, Nanjing, China. ²Atmospheric Science Program, Department of Geography, Ohio State University, Columbus, OH, USA. ³Department of Atmospheric and Oceanic Sciences, University of Wisconsin-Madison, Madison, WI, USA. ⁴Climate and Global Dynamics Laboratory, National Center for Atmospheric Research, Boulder, CO, USA. *e-mail: he.1519@osu.edu; liu.7022@osu.edu

LETTERS NATURE CLIMATE CHANGE

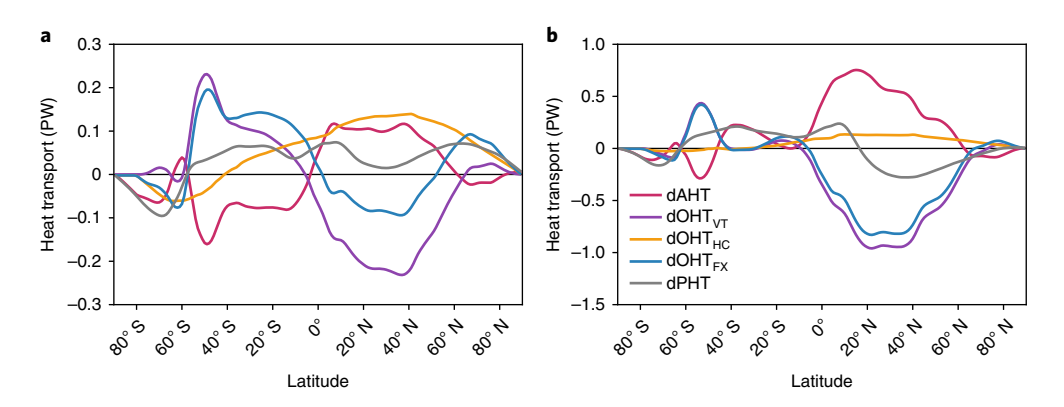


Fig. 1 | Changes in meridional heat transport between an historical CCSM4 run for 1900–2000 and CCSM4 RCP8.5 runs for the twenty-first and twenty-sixth centuries. a,b, Responses of AHT, OHT_{FX}, OHT_{VT}, OHT_{HC} and total meridional heat transport (PHT) in the twenty-first century (a; 2006–2100) and twenty-sixth century (b; 2500–2600).

consistent with previous studies^{1–3}. The poleward OHT_{VT} also shows an equatorward anomaly in both hemispheres, which is, nevertheless, distorted away from the symmetric OHT_{FX} such that the OHT_{VT} response is substantially stronger in the Northern Hemisphere than in the Southern Hemisphere (Figs. 1a and 2b). The difference between OHT_{FX} and OHT_{VT} is an apparent OHT_{HC} : $OHT_{HC} = OHT_{FX} - OHT_{VT}$, which is generated by the inhomogeneous heat storage response associated with subsurface warming $(\frac{\partial \theta}{\partial t} \gg 0)$; see equation (3) in the Methods) and has a magnitude comparable to OHT_{FX} (Fig. 1a). This OHT_{HC} anomaly increases northward from the Southern Ocean into the Northern Hemisphere mid- and high latitudes, predominately in the Indo-Pacific basin (Supplementary Fig. 2a), and then into the Arctic Ocean, mainly in the North Atlantic (Supplementary Fig. 2c).

The AHT response during the initial warming has been studied extensively^{1,2,22}. The poleward AHT is enhanced by the increased transport of dry static energy transport (DSET; see Methods) out of the tropics through the Hadley Cell, then latent energy transport (LET; see Methods) further poleward by eddy mixing. Physically, global warming increases surface evaporation of water vapour into the lower atmosphere, especially over the warm ocean in the tropics, which then increases the latent heat convergence towards the equator in the lower branch of the Hadley Cell and, eventually, the deep convection in the deep tropics. The increased convection increases the depth of the Hadley Circulation and reduces the lapse rate, both favouring a greater export of DSET, which overcompensates for the impact of the reduced Hadley Cell on AHT, leading to an enhanced AHT towards the extratropics (Supplementary Fig. 3b). The enhanced moisture over the subtropical ocean is further transported poleward in mid-latitude eddies to enhance the LET, which overwhelms the reduced DSET flux and enhances the poleward AHT in the mid-latitude in both hemispheres^{1,23,24} (Supplementary Fig. 3a).

Compared with AHT, few studies have investigated the mechanism of the OHT response during the initial warming stage. Most previous studies simply inferred the OHT response from surface heat flux as $\text{OHT}_{\text{FX}}^{1-3}$. However, OHT_{FX} differs significantly from OHT_{VT} in the initial warming stage because of the large change in heat storage, as shown in Fig. 1a. Here, we focus on the response of OHT_{VT} and its relationship with OHT_{FX} . OHT_{VT} is reduced in both hemispheres (compensating for the AHT response) mainly by the weakening of the cell heat transport associated with the overturning STC and AMOC (see Methods; Fig. 3a). A further decomposition (see Methods) of the cell heat transport into the advection by the mean circulation on temperature anomaly (VdT) and the advection by the circulation anomaly on mean temperature (TdV) shows

that the cell transport change is dominated by the reduced circulation (Fig. 3d; except over the Southern Ocean beyond ~50°S; see 'Mechanisms' in the Supplementary Information).

Over the Indo-Pacific basin (Fig. 3b), the reduced trade wind associated with the less vigorous Hadley Cell and Walker Cell²⁵ (Fig. 2c) weakens the upper ocean STC26 and, in turn, its poleward OHT (TdV) (Fig. 3e and Supplementary Fig. 4b). The stronger surface warming increases oceanic stratification, leading to an increased poleward OHT by the mean STC (VdT) (Fig. 3e and Supplementary Fig. 4a). This reduced OHT by TdV overwhelms the increased poleward OHT by VdT, resulting in a reduction of the total cell OHT. This OHT response is opposite to the AHT response even though they are coupled dynamically in the Hadley Cell-STC system such that the coupled circulation weakens in both the atmosphere and the ocean²⁷ during the initial warming (Fig. 2c). This weakened circulation reduces the poleward OHT but enhances the poleward AHT, because the poleward AHT is dominated by the increased gross stability effect (VdT) while the poleward OHT is dominated by the reduced circulation effect (TdV).

Locally, the symmetric nature of the coupled Hadley Cell–STC (Supplementary Fig. 1b,c) tends to produce a heat transport response that is largely symmetric about the equator. The OHT_{VT} response is somewhat stronger in the Southern Hemisphere because of the wider total basin width there (Fig. 3b). In the Northern Hemisphere, the poleward cell OHT is reduced much more in the Atlantic (Fig. 3c,f) because the weakening AMOC^{13,14} (Fig. 2a) induces a southward OHT response across both hemispheres (*TdV*), overwhelming the increased northward OHT that is advected by the mean AMOC on the stronger warming surface water (*VdT*) (Fig. 3f and Supplementary Fig. 4a,b) and leading to a net decrease of the northward cell OHT. This southward OHT response leads to an asymmetry in the total OHT_{VT} response such that the OHT reduction is larger in the Northern Hemisphere than in the Southern Hemisphere during the initial warming (Fig. 2b).

However, this asymmetric response of southward OHT from the Atlantic is partially cancelled by a northward OHT response in the apparent OHT $_{\rm HC}$ such that OHT $_{\rm EX}$ becomes largely symmetric about the equator (Fig. 1a). This northward OHT $_{\rm HC}$ response is caused by an increase in ocean heat content in the Southern Ocean during initial global warming (Fig. 4a and Supplementary Fig. 5d). In contrast with the surface air temperature (SAT) response, which is characterized by the polar amplification in the Arctic during the initial global warming (Supplementary Fig. 5a), the sea surface temperature (SST) and ocean heat content (Fig. 4a) increase more over the Southern Hemisphere (Supplementary Fig. 5c,d), with a primary peak just north of 50° S around the Antarctica Circumpolar Current

NATURE CLIMATE CHANGE LETTERS

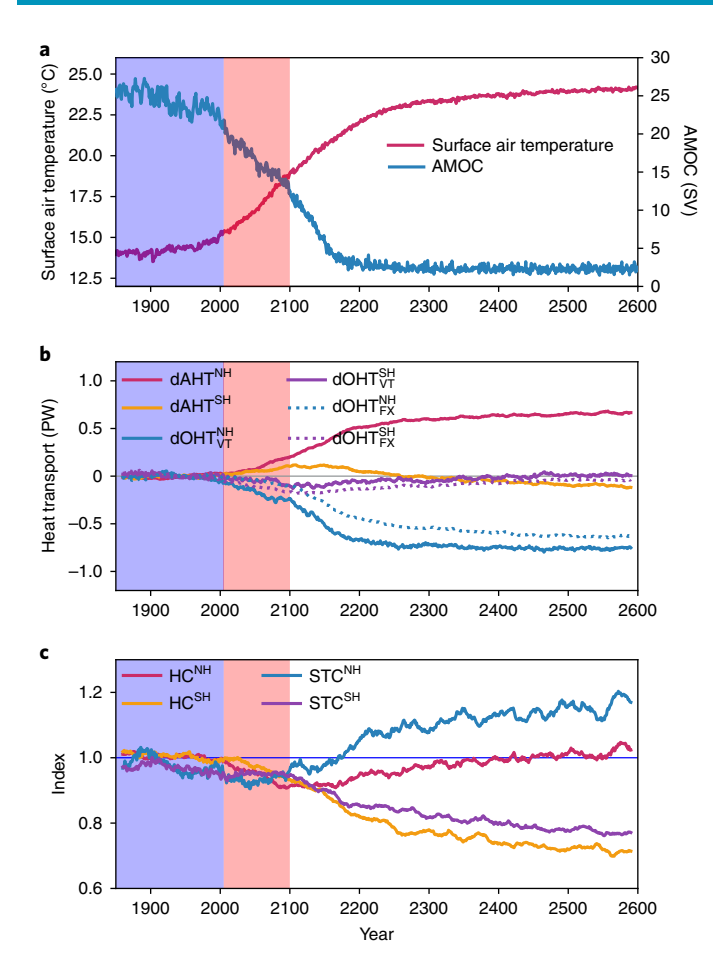


Fig. 2 | Evolution of climate from the pre-industrial era (1850) to the end of the twenty-sixth century (2600). a, Temporal evolution of global mean surface air temperature and the AMOC index in a historical run (blue shading, 1850-2005), RCP8.5 scenarios (red shading, 2006-2100) and RCP8.5 extension to 2600, with all forcing kept constant after the year 2300. **b**, As in **a**, but for average AHT and OHT anomalies in the Northern Hemisphere (NH, 0-30° N) and Southern Hemisphere (SH, 0-30° S). The anomalous AHT, OHT_{VT} and OHT_{FX} values are multiplied by -1 in the Southern Hemisphere, such that positive (negative) signs indicate poleward (equatorward) transport in both hemispheres. The apparent OHT_{HC} can be derived as the difference between the OHT_{FX} (dashed line) and OHT_{VT} (solid line). c, As in a, but for the Hadley Cell (HC) index and STC index in both hemispheres. The curves in **b** and **c** are smoothed by a 21-year running mean for illustration. See the Methods for further definitions of the indices of the average AHT and OHT anomalies and circulation. (SV, sverdrup; $1SV=1e^{6}m^{3}s^{-1}$).

(ACC) (Fig. 4b). This ocean warming centre is caused by the northward mean surface current over the ACC region (Fig. 3d), which transports energy northward due to the maximum surface heat uptake over the ACC (along ~55°S) (Supplementary Fig. 5b), forming the warming centre north of 50°S^{29,30} (Supplementary Fig. 5d). The warming centre around the Southern Ocean is actually even larger than it appears in the zonal mean heat content if we consider the total heat content integrated zonally across the entire ocean, because of the wider oceanic areas in the Southern Hemisphere (Fig. 4b,c). The warming centre around the Southern Ocean can be thought of as equivalent to a divergence of a northward apparent OHT_{HC} as follows. Assuming the OHT_{VT} remains unchanged, relative to the global mean heat storage, the region of excessive ocean heat storage represents the region of ocean heat uptake from the

atmosphere through a downward surface heat flux, and this surplus of heat can potentially be 'transported' into the region of deficient ocean heat storage and eventually to the atmosphere.

It should be pointed out that this ocean warming centre around the Southern Ocean, and the resultant northward OHT_{HC} during initial global warming, is a robust feature across climate models, such as the CESM-LE simulations (Supplementary Fig. 6) and CMIP5 simulations (Supplementary Fig. 7), and is also consistent with the recent ocean warming trend observed since 1955 (Fig. 4e-h; see Methods)^{29,31,32}. Therefore, this northward apparent OHT_{HC} response appears to cancel the southward OHT_{VT} responses associated with the weakening AMOC in the initial stage of global warming, leading to a largely symmetric OHT_{EX} that appears to compensate for the increased poleward AHT globally, as seen in previous studies¹⁻³. From the oceanic perspective, physically, this reflects an asymmetric oceanic response to an initial symmetric surface heating at high latitudes. Over the North Atlantic, the surface warming penetrates deep (Supplementary Fig. 4a), weakening the AMOC^{13,15} and, in turn, produces a southward OHT_{VT} response all the way into the Southern Hemisphere. Over the Southern Ocean, the surface warming is trapped in the upper ocean locally (Supplementary Fig. 4), with no significant impact on ocean circulation, thus creating a Southern Ocean warming centre that corresponds to apparent OHT_{HC} northward. One notices that OHT_{EX}, albeit largely symmetric about the equator, shows a small crossequator component in CMIP5 and CESM-LE. This small crossequator OHT_{FX} is caused mostly by the cross-equatorial OHT_{VT} in the Atlantic due to the different model sensitivity of the AMOC to global warming (Supplementary Figs. 6c and 7c).

However, this symmetric heat transport response in the twentyfirst century is altered significantly to a largely asymmetric response later in the following centuries, when the CO₂ concentration levels off and the coupled system approaches a quasi-equilibrium state after the deep ocean adjustment (Fig. 2a). During this later stage of global warming, the AMOC continues to decline to its minimum at ~2200 (Fig. 2a). The further decline of the AMOC induces further southward OHT_{VT} in both hemispheres, which enhances the southward OHT_{VT} anomaly in the Northern Hemisphere and opposes the northward OHT_{VT} anomaly triggered by further reduced STCs in the Southern Hemisphere (Fig. 2c), eventually leading to diminishing OHT_{VT} (Fig. 2b). Furthermore, the approach towards quasiequilibrium leads to a significant reduction of the contribution of the oceanic heat storage effect, or OHT_{HC}, relative to the growing OHT_{VT} such that almost all OHT_{VT} is fluxed to the atmosphere through OHT_{EX} (Fig. 2b). This leads to compensatory AHT^{9,33} that is significantly enhanced in the Northern Hemisphere but diminishes in the Southern Hemisphere (Fig. 2b). As a result, the heat transport exhibits an inter-hemispherically asymmetric and compensating response in the Northern Hemisphere and little heat transport in the Southern Hemisphere (Fig. 1b; also see the Supplementary Information). This tendency from an initial symmetric response towards a later asymmetric response is consistent with recent work¹⁷ and is also likely to be valid in most other models, because most models have shown a continued decline of the AMOC with further global warming in the RCP8.5 scenario^{3,13,15}, and the ocean should approach quasi-equilibrium with additional adjustment times.

In summary, our study shows two distinct features of the heat transport response in the initial warming stage. First, the initial weakening of AMOC induces a southward heat transport response OHT_{VT} across the equator in the Atlantic. However, this inter-hemispherically asymmetric OHT response appears to be cancelled by a northward apparent OHT_{HC} that is dominated by ocean warming centred near the Southern Ocean. Second, the coupled Hadley Cell–STC exhibits a largely inter-hemispherically symmetric response in the tropics, with a reduced OHT_{VT} associated with the weakening of the STC (TdV), compensated for by an enhanced poleward AHT

LETTERS NATURE CLIMATE CHANGE

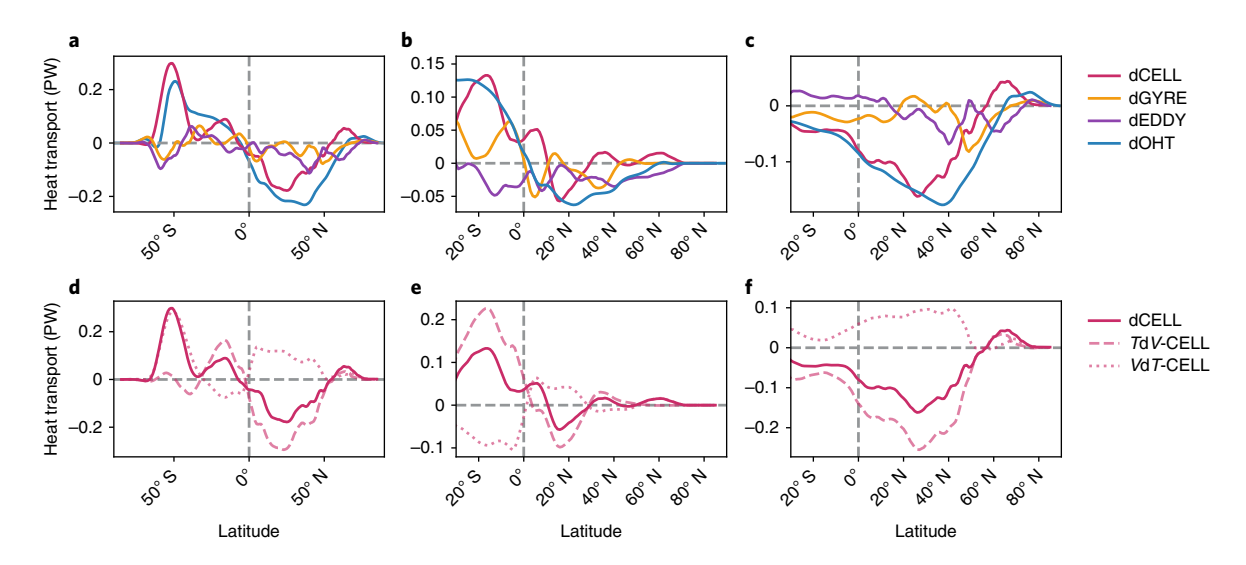


Fig. 3 | Response of OHT between historical (1900–2000) and twenty-first-century RCP8.5 runs (2006–2100) of the coupled CCSM4 model. a-c, Anomalous total OHT (blue) and its components (that is, cell OHT (red), gyre OHT (orange) and eddy OHT (purple)) globally (a), in the Indo-Pacific basin (b) and in the Atlantic basin (c). **d-f**, The changes in cell OHT shown in **a-c** are further partitioned into heat transports by circulation change (*TdV*-CELL, dashed) and temperature change (*VdT*-CELL, dotted), respectively.

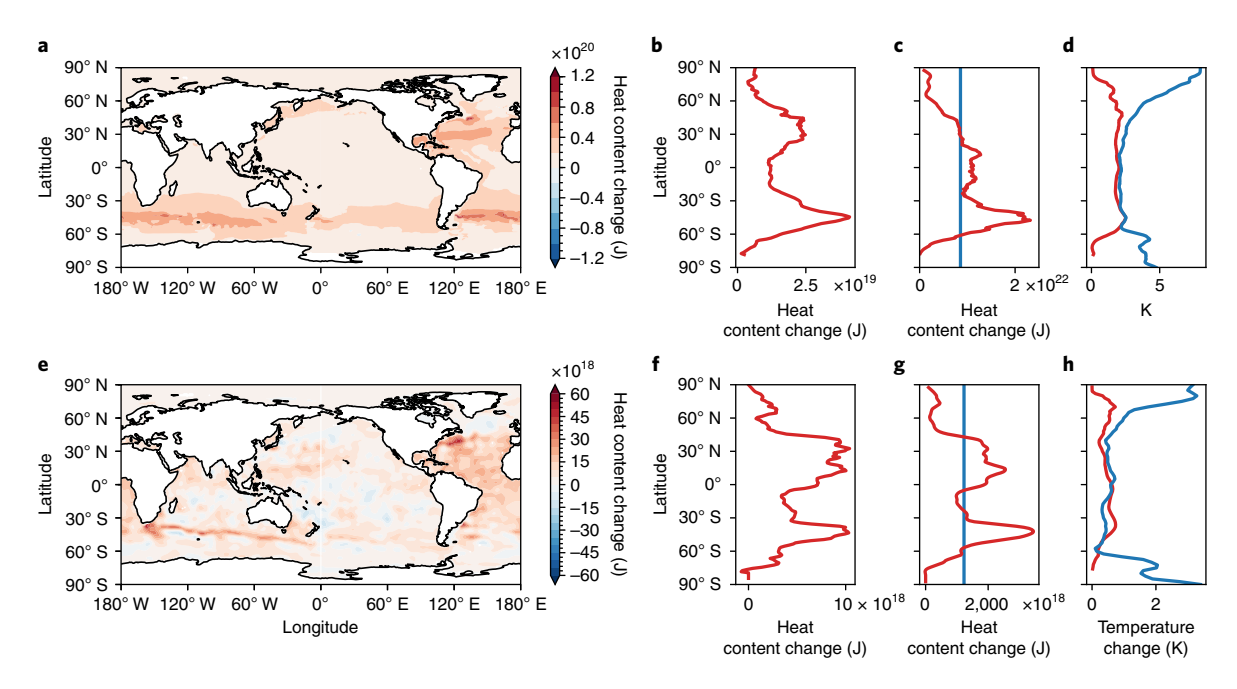


Fig. 4 | Ocean heat content and temperature change, as calculated from CCSM4 modelling and observations. a-d, CCSM4-modelled ocean heat content and temperature change in the twenty-first century (2006–2100) relative to the historical run (1900–2000), shown as vertical integration (a), a zonal average (b), zonal integration (c), and zonal mean SAT (blue) and SST (red) (d). e-h, As in a-d, respectively, but using observational data. In e-g, the heat content anomaly was calculated as the difference between climatologies of 2000–2017 and 1955–1975 for a depth of 0–2,000 m. In h, the SAT and SST anomalies were derived in the same period as in e-g. In c and g, the blue vertical lines correspond to the global mean of total heat uptake by the ocean.

due to the increased gross stability (VdT). As such, the symmetric and compensated response between OHT $_{\rm FX}$ and AHT is mainly expressed in the coupled Hadley Cell–STC. However, this initial symmetric and compensated heat transport response is likely to be altered in the following centuries in a quasi-equilibrium state to an asymmetric compensation response^{17,33}, largely confined in the Northern Hemisphere.

Overall, our study suggests that the large OHT_{HC} in the initial warming stage leads to OHT_{FX} that is significantly different from

OHT_{VT}. This understanding of the coupled heat transport response is important for understanding the future response of global climate processes, such as the uptake and redistribution of ocean heat²⁹ and the shift of the atmospheric Intertropical Convergence Zone³⁴. However, further studies are still needed. In particular, the explicit OHT should be studied in other models. Additionally, OHT needs to be studied in the next generation of models that resolve ocean eddies, whose effect may have been underestimated in current non-eddy-resolving models. Furthermore, longer simulations of

NATURE CLIMATE CHANGE LETTERS

thousands of years are also needed to examine the final equilibrium state, when the AMOC may recover^{17,35} and lead to yet another different heat transport response.

Online content

Any methods, additional references, Nature Research reporting summaries, source data, statements of data availability and associated accession codes are available at https://doi.org/10.1038/s41558-018-0387-3.

Received: 14 August 2018; Accepted: 5 December 2018; Published online: 28 January 2019

References

- Held, I. & Soden, B. J. Robust response of the hydrological cycle to global warming. J. Clim. 19, 5686–5699 (2006).
- Zelinka, M. D. & Hartmann, D. L. Climate feedbacks and their implications for poleward energy flux changes in a warming climate. *J. Clim.* 25, 608–624 (2012).
- Hu, A., Meehl, G. A., Han, W., Lu, J. & Strand, W. G. Energy balance in a warm world without the ocean conveyor belt and sea ice. *Geophys. Res. Lett.* 40, 6242–6246 (2013).
- Ganachaud, A. & Wunsch, C. Improved estimates of global ocean circulation, heat transport and mixing from hydrographic data. *Nature* 408, 453–457 (2000).
- Collins, M. et al. Challenges and opportunities for improved understanding of regional climate dynamics. *Nat. Clim. Change* 8, 101–108 (2018).
- Hwang, Y. T. & Frierson, D. M. W. Increasing atmospheric poleward energy transport with global warming. *Geophys. Res. Lett.* 37, 1–5 (2010).
- 7. Bjerknes, J. Atlantic air-sea interaction. Adv. Geophys. 10, 1-82 (1964).
- Zhao, Y., Yang, H. & Liu, Z. Assessing Bjerknes compensation for climate variability and its time-scale dependence. *J. Clim.* 29, 5501–5512 (2016).
- Liu, Z. et al. Local and remote responses of atmospheric and oceanic heat transports to climate forcing: compensation versus collaboration. J. Clim. 31, 6445–6460 (2018).
- Yang, H., Zhao, Y. & Liu, Z. Understanding Bjerknes compensation in atmosphere and ocean heat transports using a coupled box model. *J. Clim.* 29, 2145–2160 (2016).
- Gleckler, P. J., Durack, P. J., Stouffer, R. J., Johnson, G. C. & Forest, C. E. Industrial-era global ocean heat uptake doubles in recent decades. *Nat. Clim. Change* 6, 394–398 (2016).
- 12. Federation, K. R. & Lynne, D. in *Climate Change 2013: The Physical Science Basis* (eds Stocker, T. F. et al.) 255–316 (IPCC, Cambridge Univ. Press, 2013).
- Gregory, J. M. et al. A model intercomparison of changes in the Atlantic thermohaline circulation in response to increasing atmospheric CO₂ concentration. *Geophys. Res. Lett.* 32, 1–5 (2005).
- Sévellec, F., Fedorov, A. V. & Liu, W. Arctic sea-ice decline weakens the Atlantic Meridional Overturning Circulation. *Nat. Clim. Change* 7, 604–610 (2017).
- 15. Weaver, A. J. et al. Stability of the Atlantic Meridional Overturning Circulation: a model intercomparison. *Geophys. Res. Lett.* **39**, 1–8 (2012).
- Yang, H., Wang, Y. & Liu, Z. A modelling study of the Bjerknes compensation in the meridional heat transport in a freshening ocean. *Tellus A* 65, 1–8 (2013).
- 17. Yang, Q. et al. Understanding Bjerknes compensation in meridional heat transports and the role of freshwater in a warming climate. *J. Clim.* **31**, 4791–4806 (2018).
- 18. Kang, S. M., Held, I. M., Frierson, D. M. W. & Zhao, M. The response of the ITCZ to extratropical thermal forcing: idealized slab-ocean experiments with a GCM. *J. Clim.* 21, 3521–3532 (2008).
- Gent, P. R. et al. The Community Climate System Model version 4. *J. Clim.* 24, 4973–4991 (2011).
- Kay, J. E. et al. The Community Earth System Model (CESM) Large Ensemble project: a community resource for studying climate change in the presence of internal climate variability. *Bull. Am. Meteorol. Soc.* 96, 1333–1349 (2015).
- Taylor, K. E., Stouffer, R. J. & Meehl, G. A. An overview of CMIP5 and the experiment design. Bull. Am. Meteorol. Soc. 93, 485–498 (2012).
- Lu, J. & Cai, M. Quantifying contributions to polar warming amplification in an idealized coupled general circulation model. *Clim. Dynam.* 34, 669–687 (2010).

- 23. Shaw, T. A. et al. Storm track processes and the opposing influences of climate change. *Nat. Geosci.* **9**, 656–664 (2016).
- Chang, E. K. M., Guo, Y. & Xia, X. CMIP5 multimodel ensemble projection of storm track change under global warming. *J. Geophys. Res. Atmos.* 117, 1–19 (2012).
- 25. Vecchi, G. A. et al. Weakening of tropical Pacific atmospheric circulation due to anthropogenic forcing. *Nature* **441**, 73–76 (2006).
- Liu, Z., Philander, S. G. H. & Pacanowski, R. C. A GCM study of tropical-subtropical upper-ocean water exchange. *J. Phys. Oceanogr.* 24, 2606–2623 (1994).
- Held, I. M. The partitioning of the poleward energy transport between the tropical ocean and atmosphere. J. Atmos. Sci. 58, 943–948 (2001).
- Back, L. et al. Global hydrological cycle response to rapid and slow global warming. J. Clim. 26, 8781–8786 (2013).
- Armour, K. C., Marshall, J., Scott, J. R., Donohoe, A. & Newsom, E. R. Southern Ocean warming delayed by circumpolar upwelling and equatorward transport. *Nat. Geosci.* 9, 549–554 (2016).
- Liu, W., Lu, J., Xie, S.-P. & Fedorov, A. Southern Ocean heat uptake, redistribution and storage in a warming climate: the role of meridional overturning circulation. J. Clim. 31, 4727–4743 (2018).
- Levitus, S. et al. World ocean heat content and thermosteric sea level change (0–2000m), 1955–2010. Geophys. Res. Lett. 39, 1–5 (2012).
- 32. Roemmich, D. et al. Unabated planetary warming and its ocean structure since 2006. *Nat. Clim. Change* 5, 240–245 (2015).
- Liu, Z., Yang, H., He, C. & Zhao, Y. A theory for Bjerknes compensation: the role of climate feedback. J. Clim. 29, 191–208 (2016).
- Green, B. & Marshall, J. Coupling of trade winds with ocean circulation damps ITCZ shifts. J. Clim. 30, 4395–4411 (2017).
- 35. Jansen, M. F., Nadeau, L. P. & Merlis, T. M. Transient versus equilibrium response of the ocean's overturning circulation to warming. *J. Clim.* **31**, 5147–5163 (2018).

Acknowledgements

This work is supported by MOST 2017YFA0603801, NSFC41630527, NSF1656907, NSF1810682 and the Nanjing University of Information Science and Technology. We thank Q. Li and J. Han for a discussion on meridional heat transport calculation in CCSM4, and L. Franchisteguy, A. Voldoire and H. Haak for discussions on meridional heat transport calculations in CMIP5 models. We acknowledge the climate modelling groups for producing model outputs, the Program for Climate Model Diagnosis and Intercomparison for maintaining the CMIP5 data archive from which we drew the data, and the CESM community for providing the CESM-LE product. We also acknowledge the high-performance computing support from NCAR's Computational and Information Systems Laboratory, sponsored by the National Science Foundation. Portions of this study are supported by the Regional and Global Model Analysis component of the Earth and Environmental System Modeling programme of the US Department of Energy's Office of Biological and Environmental Research Cooperative Agreement number DE-FC02-97ER62402, and the National Science Foundation. This research also uses resources of the National Energy Research Scientific Computing Center supported by the Office of Science of the US Department of Energy under contract number DE-AC02-05CH11231. Finally, this work could not have been completed without xcesm—a decent Python package (https://github.com/Yefee/xcesm) based on Xarray (http://xarray.pydata. org/en/stable/) for CESM output diagnosis.

Author contributions

C.H. and Z.L designed the study. C.H. performed the analysis. A.H. provided CESM simulation data. Z.L. and C.H. wrote the manuscript with input from A.H.

Competing interests

The authors declare no competing interests.

Additional information

Supplementary information is available for this paper at $\rm https://doi.org/10.1038/s41558-018-0387-3$.

Reprints and permissions information is available at www.nature.com/reprints.

Correspondence and requests for materials should be addressed to C.H. or Z.L.

Journal peer review information *Nature Climate Change* thanks Yen-Ting Hwan and other anonymous reviewer(s) for their contribution to the peer review of this work.

Publisher's note: Springer Nature remains neutral with regard to jurisdictional claims in published maps and institutional affiliations.

© The Author(s), under exclusive licence to Springer Nature Limited 2019

LETTERS NATURE CLIMATE CHANGE

Methods

Historical and RCP8.5 runs of the coupled CCSM4 model. CCSM4 is a fully coupled climate model with an atmosphere of ~1° coupled with a nominally 1° ocean 19. We analysed the results of an historical run from 1850 to 2005 (which was forced by the observed atmospheric composition changes, as in the CMIP5 protocol 21), an RCP8.5 global warming scenario from 2005 to 2300, and an extension run from 2300 to 2600 in which all forcing was kept constant at the levels of the year 2300 (ref. 3). The global mean temperature largely follows the CO₂ forcing, warming by ~10°C to reach a quasi-equilibrium by 2300. Accompanied by the polar amplification in surface air temperature, subpolar SST keeps rising, with the Southern Ocean taking much more heat than other latitudes (Fig. 4a,c). More details on the model evolution are discussed in ref. 3 .

CESM-LE simulations. The CESM community produces a large ensemble (40 members) using a nominal \sim 1° CESM with diagnostic biogeochemistry calculations for the ocean ecosystem and atmospheric carbon dioxide cycle²⁰. Each ensemble runs from 1920–2100 using historical forcing (1920–2005) and RCP85 (2006–2100), but with slightly different initial conditions. Here, we use the first 30 members to analyse the response of AHT and OHT (below) between its historical runs (1920–2000) and RCP8.5 runs (2020–2100).

OHT response in CMIP5 models. The historical simulations (1981–2000) and RCP8.5 experiments (2081–2100) from 15 coupled general circulation models (CGCMs) from CMIP5 are analysed. The model information is shown in Supplementary Table 1. Note that the CMIP5 archive does not provide enough variables to compute the OHT $_{\rm VT}$ based on equation (2), so the OHT $_{\rm VT}$ here is calculated as the residual of OHT $_{\rm FX}$ and OHT $_{\rm HC}$ and OHT $_{\rm FX}$ and OHT $_{\rm HC}$ are computed according to equation (1) and (3), which will be discussed later.

Observations. The global ocean heat content anomaly from 1955–2017 for a depth of 0–2,000 m was obtained from the National Oceanic and Atmospheric Administration's Climate Data Record³¹. The heat content change was calculated from the data gathered from the National Centers for Environmental Information archives, which are uniformly formatted and quality controlled in the World Ocean Database (https://www.nodc.noaa.gov/OC5/WOD/pr_wod.html). SST and SAT anomalies were obtained, respectively, from the National Oceanic and Atmospheric Administration's Extended Reconstructed Sea Surface Temperature version 5 (ref. ³⁶) and National Centers for Atmospheric Prediction/NCAR Reanalysis 1 (ref. ³⁷) during the same period.

OHT. The OHT can be conveniently calculated, as in most previous studies on global warming, by integrating the net surface heat flux Q_0 (after removing the global mean) from the South Pole (at $\phi = \phi_s$) as:

$$OHT_{FX}(\phi) = c_p \rho_0 \int_{\lambda_F}^{\lambda_W} \int_{\phi_c}^{\phi} Q_0 \cos\phi d\phi d\lambda$$
 (1)

where $c_{\rm p}$ and $\rho_{\rm 0}$ are the specific heat and density of the sea water, respectively, and $\lambda_{\rm E}$ and $\lambda_{\rm W}$ are the eastern and western boundaries of the ocean basin, respectively. This OHT $_{\rm FX}$ is the true OHT $_{\rm VT}$ only if the ocean is in the equilibrium state (Supplementary Fig. 1a). However, since the global warming response exhibits significant transient behaviour (Fig. 2), the OHT $_{\rm FX}$ can differ significantly from the true OHT $_{\rm VT}$ can be calculated directly in the advective temperature flux with the Redi isoneutral diffusion term $R(\theta)$ as:

$$\begin{aligned} \text{OHT}_{\text{VT}}(\phi) &= c_{\text{p}} \rho_{0} \int_{-H}^{0} \int_{\lambda_{\text{E}}}^{\lambda_{\text{W}}} v \theta \text{cos} \phi \text{d} \lambda \text{d} z \\ &+ c_{\text{p}} \rho_{0} \int_{\phi_{\text{c}}}^{\phi} \int_{-H}^{0} \int_{\lambda_{\text{E}}}^{\lambda_{\text{W}}} R(\theta) \text{d} \phi \text{d} \lambda \text{d} z \end{aligned} \tag{2}$$

where ν and θ are the total meridional velocity (Eularian mean plus eddy induced) and potential temperature of the ocean, respectively, and the temperature transport is integrated from the bottom (-H) to the surface along the vertical coordinate z. The difference between OHT_{FX} and OHT_{VT} is due to the effect of OHT_{HC} : $OHT_{FX} - OHT_{VT} = OHT_{HC}$ which can also be calculated directly as:

$$OHT_{HC}(\phi) = c_p \rho_0 \int_{-H}^{0} \int_{\lambda_E}^{\lambda_W} \int_{\phi_S}^{\phi} \frac{\partial \theta}{\partial t} \cos\phi d\phi d\lambda dz$$
 (3)

As in the case of $\mathrm{OHT}_{\mathrm{FX}}$, the global mean has been subtracted from the heat storage $\frac{\partial \theta}{\partial t}$ in equation (3). It should be noted that the $\mathrm{OHT}_{\mathrm{HC}}$ thus defined can be thought of as an equivalent $\mathrm{OHT}_{\mathrm{VT}}$ caused by the same surface heat flux. For example, localized surface heating forces local ocean warming and this warming can be thought of as equivalent to a divergence of $\mathrm{OHT}_{\mathrm{VT}}$ of the same magnitude.

AHT. The meridional AHT at latitude ϕ is calculated by integrating the net heat flux into the atmosphere (after removing the global mean) from the South Pole (at $\phi = \phi_s$) as:

$$AHT(\phi) = a_E^2 \int_{\phi_c}^{\phi} \int_0^{2\pi} (Q_{TOA} - Q_0) \cos\phi d\lambda d\phi$$
 (4)

where Q_{TOA} and Q_0 are the net incoming radiation at the TOA and the net surface heat flux, respectively, and a_{E} and λ are the radius of the earth and longitudes in radian. The LET can be integrated using CCSM4 monthly model output $v_{\text{a}}q$ (meridional moisture flux) along the pressure coordinate:

$$LET(\phi) = \frac{a_E}{g} l_v \int_0^{2\pi} \int_0^{p_s} v_u q \cos\phi \, dp d\lambda$$
 (5)

in which l_v and g are the latent heat of vaporization and standard gravity. Finally, the DSET can be derived as the residual of AHT and LET.

Decomposition of OHT_{VT} with regard to ocean circulation. The OHT_{VT} in each basin can be decomposed into subcomponents associated with cells, gyres and eddy transport as:

$$[\overline{\nu\theta}] = [\overline{(\nu_{\text{eul}} + \nu_{\text{bol}})\theta}] = [\overline{\nu_{\text{eul}}}] [\overline{\theta}] + [\overline{\nu_{\text{eul}}}^* \overline{\theta}^*] + [\overline{\nu_{\text{eul}}'\theta'}] + [\overline{\nu_{\text{bol}}\theta}]$$
(6)

The total meridional velocity is decomposed into the Eulerian mean and bolus velocity induced by eddies. An overbar and a prime denote the time average and its deviation, respectively, while a bracket and an asterisk denote the zonal mean and its departure. The first term on the right-hand side is the heat transport by overturning circulation cells (or, simply, cell hereafter). This is accomplished mainly by the STC in the upper Indian and Pacific Ocean and by the AMOC in the Atlantic. The second term on the right-hand side is the heat transport by horizontal gyres, such as the warm poleward western boundary current and the cold returning flow in the interior basin and eastern boundary in a subtropical gyre. The last two terms on the right-hand side are transient variability induced heat transport and eddy heat transport parameterized in the Gent-McWillimas scheme³⁸. They are usually small, and we combine them with the diffusion term in equation (2) and call the combined term 'eddy OHT'. This term will not be discussed here because it is small in general, except over the Southern Ocean and strong western boundary currents where eddy activity is non-negligible. The OHT_{VT} defined in equation (2) was obtained by integrating all terms in equation (6) vertically, plus the diffusion term $R(\theta)$ -induced OHT. Since the CCSM4 ocean model is in curvilinear grids, we re-grid the rotated Eulerian velocity and temperature to high-resolution Cartesian grids, then integrate their product horizontally and vertically as the first term on the right-hand side of equation (2). Finally, we perform a latitudinal smooth to obtain OHT latitudinal profiles by different ocean circulations. The $\nu\theta$ -constructed OHT shows excellent consistency with that of the model output.

Decomposition of OHT anomaly. The OHT anomaly (dVT) can always be decomposed into two parts (VdT and TdV) due to the equation dVT = VdT + TdV.

Average AHT and OHT anomalies in the Northern and Southern hemispheres. The AHT and OHT anomalies in Fig. 2b were calculated by averaging the AHT and OHT responses in 0–30° S and 0–30° N. This latitude belt was chosen because significant heat transport responses are produced in this region, and it includes the Hadley Cell–STC (Supplementary Fig. 1b).

General overturning circulation index. The AMOC index is defined as the maximum values of streamfunction below 500 m over 40–80° N in the Atlantic following ref. 3 . The Indo-Pacific STC strength index is defined as the average of the first 2% of maximum values of the streamfunction in the Indo-Pacific basin from the surface to 500 m over 0–30° N (STC $^{\rm NH}$) and 0–30° S (STC $^{\rm SH}$), and normalized by its climatology in 1900–2000. Similarly, the Hadley Cell index is defined as the average of the first 1% of maximum values of the streamfunction in the Northern Hemisphere (HC $^{\rm NH}$) and Southern Hemisphere (HC $^{\rm SH}$), and normalized by its climatology in 1900–2000.

Data availability

The CMIP5 data used in this study can be downloaded from the Program for Climate Model Diagnosis and Intercomparison (http://cmip-pcmdi.llnl.gov/cmip5/data_portal.html). The CESM-LE data can be found at http://www.cesm.ucar.edu/projects/community-projects/LENS/. The CCSM4 data and the data supporting the findings of this study are available from the corresponding author upon request.

References

- Huang, B. et al. Extended Reconstructed Sea Surface Temperature, version 5 (ERSSTv5): upgrades, validations, and intercomparisons. *J. Clim.* 30, 8179–8205 (2017).
- Kalnay, E. et al. The NCEP/NCAR 40-year reanalysis project. Bull. Am. Meteorol. Soc. 77, 437–471 (1996).
- Gent, P. R. & Mcwilliams, J. C. Isopycnal mixing in ocean circulation models. J. Phys. Oceanogr. 20, 150–155 (1990).